Neck Injury Risk Curve Development for THOR-AV 50th Percentile Male Dummy

Z. Jerry Wang, George Hu

Abstract Neck injury risk curves were investigated for the THOR-AV dummy, a modified THOR dummy designed to represent both upright and reclined occupant postures. Isolated head/neck PMHS tests were identified and selected for this study. The PMHS injury status was paired with the corresponding neck force and moment data from the finite element simulations with THOR-AV to develop injury risk curves (IRCs). IRCs were generated for neck compression force (Fz), flexion moment at the occipital condyle (Myoc), and Nij. The critical values for Fz and Myoc were determined based on the injury assessment risk values (IARVs) at the 50% injury risk level for AIS2+. The IARVs at 5%, 25%, and 50% injury risk levels for neck compression, neck flexion, and Nij are presented in this paper. Due to insufficient data for neck tension and/or extension, no IARVs for these conditions were recommended in this study.

Keywords Dummy, Injury Risk Curve, neck, Nij, THOR-AV.

I. INTRODUCTION

Test device for Human Occupant Restraint for Automated Vehicles (THOR-AV), a modified THOR anthropomorphic test device (ATD), was designed to represent the sitting postures of a 50th percentile male in both upright and reclined positions. The development of the THOR-AV began in 2018 at the request of the automotive industry to address occupant safety in vehicles equipped with automated driving systems (ADS), where occupants may adopt various postures for relaxation, work, or social interaction [1].

Currently, vehicle safety regulations only assess upright postures, leaving occupant safety in non-traditional postures largely unknown. The THOR-AV has undergone biofidelity evaluation in 17 different sled test configurations [2]-[5], demonstrating “good” to “excellent” biofidelity under these conditions. Meanwhile, the China Automotive Engineering and Research Institute (CAERI) has been developing a test protocol for zero-gravity seats in the Chinese automotive market. In December 2024, CAERI announced the selection of the THOR-AV for its test protocol to assess the safety of the reclined seats.

To use the THOR-AV for restraint system evaluation, injury risk curves are required to estimate injury risks and to establish thresholds for vehicle design. One study [6] presented injury risk functions for the THOR-AV dummy in the lumbar spine, abdomen, and anterior superior iliac spine (ASIS). The focus in this study, however, is on developing neck injury risk curves. The design of the other body segments in the THOR-AV is identical to that of the standard THOR dummy, allowing the use of injury risk curves for these regions previously developed by the National Highway Traffic Safety Administration (NHTSA). The objective of this research is to develop neck injury risk curves specifically for the THOR-AV.

II. METHODS

A review of isolated head-neck literature was conducted to identify post-mortem human subject (PMHS) load cases for developing neck injury risk curves. After selecting the relevant PMHS test load cases, the loading environment and boundary conditions were implemented into a finite element (FE) model. Matched-pair tests were then performed using the THOR-AV head/neck FE model to generate ATD output corresponding to the PMHS load cases. The ATD data were subsequently paired with PMHS Abbreviated Injury Scale (AIS) [7] scores under the same test conditions to develop injury risk curves for the THOR-AV neck. The following sections provide further details on this process.

Z. J. Wang (e-mail: jwang@humaneticsgroup.com; tel: +1 248 778 2133) is the Chief Technology Officer of Humanetics Innovative Solutions, Inc., USA. G. Hu is the CAE Manager of Humanetics China.

THOR-AV Neck Design

THOR-AV neck was designed to address a few issues from the existing neck designs in Hybrid III and THOR [2]. Unlike the Hybrid III and THOR neck with a straight uniform cross section, the THOR-AV neck had a human like curvature representation, a smaller cross section on the upper portion, tapered down to the bottom portion. The THOR-AV neck also has a torsion element that allows approximately 45° head rotation in left and right direction with low resistance. The side view of Hybrid III, THOR and THOR-AV 50th percentile neck designs are shown in Fig. 1.

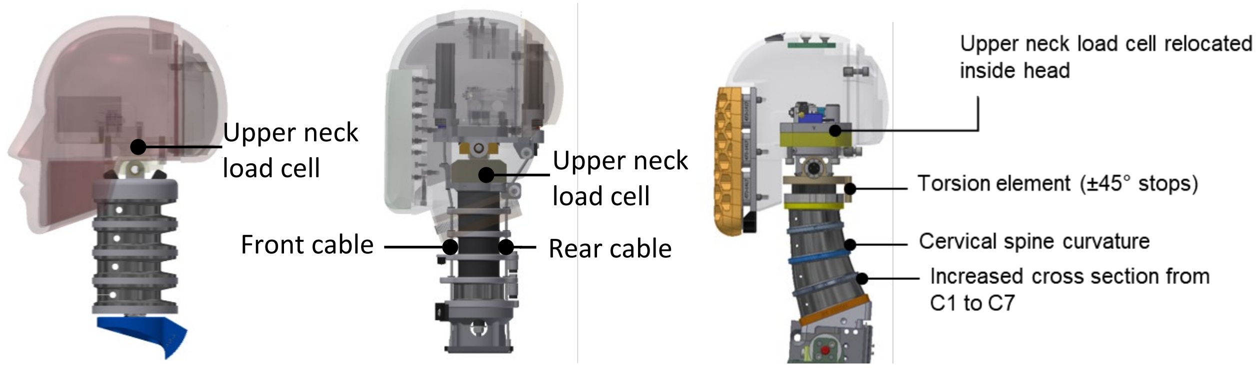

Fig. 1 Neck designs: HIII 50th (left), THOR-50M(center), THOR-AV 50M (right)

PMHS Load Case Selection

A literature review was conducted to identify publications featuring PMHS tests related to neck injury. However, many of these publications were found to be unsuitable for this research for various reasons. Partial neck tests, which involved only a single vertebra or a subset of vertebrae, were excluded because they do not accurately represent the response of the entire neck. Conversely, full-body tests focused on neck injury posed challenges in replication due to the complex initial positioning of the PMHS, especially in FE simulations where the ATD lacks the flexibility of a human body. Additionally, some publications did not provide sufficient details on boundary conditions or loading pulses, making it impossible to accurately reconstruct test conditions in the FE analysis. For example:

- Reference [8] involved a full-body test, making it a challenging load case for THOR-AV to match the PMHS initial posture.
- Reference [9] utilised a full PMHS test with neck instrumentation that compromised neck integrity, rendering the data unsuitable for this study.
- Reference [10] lacked key measurements, such as the distance from the neck centre to the clevis centre.
- References [11] and [12] did not specify the loading speed.
- Reference [13] has only one male specimen and was tested in quasi-static test condition.

After a thorough review, the selected cases are listed in Table I. Only male PMHS load cases were included in this study; female load cases were excluded but are provided in Table I for reference. The detailed list of the specimen, including age, injury status, and loading speed, is given in Table A1 in the Appendix. The scaled data are provided in Table A2 in the Appendix.

TABLE I
SUMMARY OF THE PMHS LOADING CASES

References	Segment	Loading Mode	PMHS	Loading Speed (m/s)
McElhaney *et al.* 1983 [14]	Base of the skull to T1 or C7	Compression	10 Male 4 Female	0.50–0.92
Pintar *et al.* 1989 [15]	C1 to T1	Compression	7 Male	7.5
Pintar *et al.* 1990 [16]	C1 to T1	Compression	1 Male 5 Female	8.13 2.95–7.14
Yoganandan *et al.* 1991 [17]	Full neck	Compression	4 Male 2 Female	5.4–7.8 5.3–7.3
Nightingale *et al.* 1997 [18 -19]	Head/Neck	Compression/ Flexion/Extension	17 Male 5 Female	3.1

FE Simulation

The FE model of the head and neck was validated in six loading conditions [2], which were all biofidelity test conditions. The detailed setup for each loading condition were documented in [20-22], which focused on head and neck kinematics and the lower neck load.

For the load cases selected for the analysis in this study, the fixtures that were used to mount the PMHS specimens and the impactors were modeled according to the details reported in each publication. Each PMHS specimen was simulated with the THOR-AV head-neck system with its initial impact speed for each case. The FE model was set up to match human anatomical neck level for each PMHS test. For example, if the head was included the PMHS test, the FE model included the head as well. If only the neck was included in the PMHS test, the FE model only had the neck in the analysis. If there are multiple PMHS specimens were tested in the same test condition, only one simulation was carried out. The FE results were then scaled according to the specific PMHS data to generate the data point for that specific PMHS test.

The outputs from the upper neck load cell, including forces and moments in the x-, y- and z-directions, were analysed for injury risk curve investigation.

Neck Moment Calculation at Occipital Condyle

The neck moments were transferred to the moments at occipital condyle (OC). The offset between the upper neck load cell neutral axis and the OC join is shown in Fig. 2. The following formula were used for the calculation.

Mxoc = Mx + Fy*d (1)

Myoc = My – Fx*d (2)

where d = 0.0305 meter.

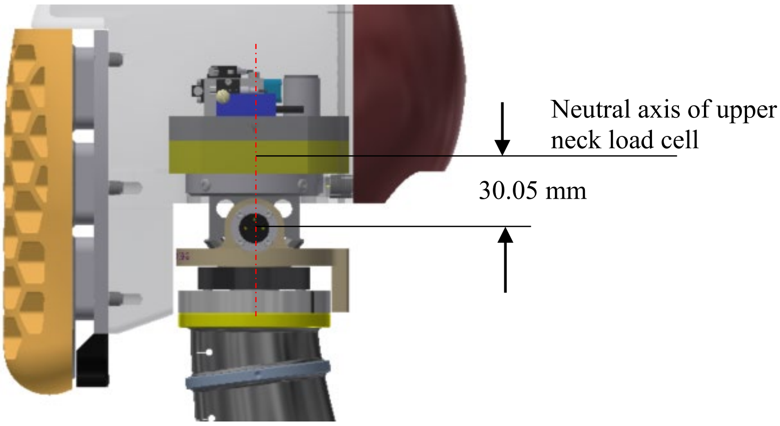

Fig. 2. THOR-AV upper neck load cell moment arm

Scaling Method

Two scaling methods were used in this study [23-24]. If both neck circumference and weight were available, the scaling method defined in [23] was applied. If only weight and stature were provided, the method outlined in [24] was used. When the necessary information for the PMHS specimens was available, the FE simulation data were scaled accordingly. Otherwise, no scaling was performed. The two scaling methods are summarised below.

Scaling method defined in [23]:
- Mass: $\lambda_M = M_s/M_{atd}$
- Dimension x: $\lambda_x = C_s/C_{atd}$
- Neck force: λ_x^2
- Neck moment: λ_x^3

Scaling method defined in [24]:
- Mass: $\lambda_M = M_s/M_{atd}$
- Neck force: ${\lambda_M}^{\frac{2}{3}}$
- Neck moment: λ_M

where *s* represents PMHS subject, and *atd* represents the anthropomorphic test device, i.e. dummy. The scaling methods used for the PMHS are summarized in Table II.

TABLE II
SUMMARY OF SCALING METHODS USED FOR THE PMHS SPECIMENS

References	Scaling method
McElhaney et al. 1983 [14]	[23]
Pintar et al. 1989 [15]	[24]
Pintar et al. 1990 [16]	[24]
Yoganandan et al. 1991 [17]	[24]
Nightingale et al. 1997 [19]	None

Survival Fit

ISO TS 18506 was followed for survival model fitting in this study [25]. The 10-step method outlined in the specification is as follows: (1) collect relevant data; (2) assign the censoring status; (3) check for a single injury mechanism; (4) estimate the coefficients; (5) identify overly influential observations; (6) check the distribution assumption; (7) choose the best distribution; (8) validate the prediction; (9) calculate 95% confidence intervals and assess their relative size; (10) check the quality index. The quality index is defined as the percentage of the width of the 95% confidence intervales over the mean at 50% injury risk. The quality index is defined as follows according to reference [25]: good" from 0 to 0.5, "fair" from 0.5 to 1, "marginal" from 1 to 1.5, "unacceptable" over 1.5.

Data censoring was evaluated for each PMHS specimens in this study. It was noticed that the time when the injuries happened was not reported for all the load cases analyzed in this research. Therefore, the PMHS specimens without injuries are treated as right censored, and the PMHS specimens with injuries are treated with left censored.

To evaluate the quality of the survival model fits, the Goodman-Kruskal Gamma (GKG), Area Under the Receiver Operating Characteristic Curve (AUROC), and Quantile-Quantile (Q-Q) plots were used. Based on a previous study [6], the Weibull distribution typically provides the best fit; therefore, this study focused exclusively on the Weibull distribution, which is defined in Equation (3). GKG is a measure of association for ordinal data, ranging from –1 to +1, indicating the strength and direction of a relationship, with higher values representing stronger associations. AUROC assesses a model's ability to distinguish between classes in binary classification, ranging from 0 to 1, where 1.0 indicates perfect classification, 0.5 indicates random guessing, and values below 0.5 suggest worse-than-random performance. The Q-Q plot is a graphical tool for comparing the distribution of the data to a theoretical distribution. If the points fall approximately along a straight line, it suggests that the data follows the specified distribution; deviations indicate potential issues such as skewness or heavy tails.

Weibull cumulative density function (CDF):

$$P(x,\alpha,\beta) = \begin{cases} 1 - e^{-\left(\frac{x}{\alpha}\right)^{\beta}}, & x \geq 0 \\ 0, & x < 0 \end{cases} \tag{3}$$

where α is the scale and β is the shape.

Nij Calculation

In this analysis, the neck compression force (Fz), upper neck moment at the occipital condyle (Myoc), and Nij were investigated for developing injury risk curves. Nij was calculated with the following formula (Eq. 4):

$$Nij = \left|\frac{Fz(t)}{Fz_{cr}}\right| + \left|\frac{Myoc(t)}{My_{cr}}\right| \tag{4}$$

where *Fz(t)* is the time-dependent axial force in the neck, *Myoc(t)* is the time-dependent moment at the occipital condyle, Fz_{cr} and My_{cr} are the critical values for the dummy neck in compression/tension force and flexion/extension moment, respectively.

Critical Values for Nij Calculation

The HIII 50th percentile neck injury criteria were documented in [26-27]. The critical values for Fz_{cr} were defined as 6807 N for tension and 6160 N for compression, while for My_{cr} the values were 310 Nm for flexion and 135 Nm for extension. Additionally, in vehicle testing with the HIII 50th dummy, the peak neck tension must not exceed 4157 N, and the peak neck compression must not exceed 4000 N.

The THOR neck injury criteria were proposed by NHTSA [28]. For Nij calculation, the critical values were scaled from the HIII 50th ATD, with Fz_{cr} set at 4200 N for tension and at 4520 N for compression, while My_{cr} was 60 Nm for flexion and 79.2 Nm for extension. However, reference [28] noted that the THOR neck was tested without front and rear cables, which invalidates direct scaling since these cables influence the neck response in vehicle certification tests. No NCAP injury thresholds were proposed in this document.

Several methods have been used in the literature to establish critical values for combined loading criteria. The Brain Injury Criteria (BrIC) [29] used IARV at 50% injury risk (AIS4+) as the threshold for angular velocity. The Combined Thoracic Index (CTI) [26] targeted IARV at 5% injury risk (AIS4+) for thorax compression, aligning with AAAM recommendations. Mean injury values [30-31] were used as thresholds for the tibia index criteria. Each method has strengths and limitations, with no clear advantage of one over the others.

The selection of critical values for combined injury criteria, such as Nij, has been inconsistent in justification. Reference [3] proposed using injury values at the 50% injury risk level for lumbar combined loading criteria (Lij) as an objective approach to determine critical values. A multiplier of 2 was applied to the values at 50% injury risk to bring Lij closer to 1.0 at this risk level; however, this normalisation factor may not be necessary.

In this study, the injury assessment reference values (IARVs) at 50% injury risk for AIS2+ were used as the critical values. The AIS2+ threshold includes more injurious cases compared to AIS3+ or higher, making it statistically more meaningful. No multiplier was used to normalise Nij to a value near 1.0 at 50% injury risk. The IARV at this risk level represents the median value within the overlap of injurious and non-injurious cases. Statistically, it is reasonable to assume that half of the sample cases result in injuries, making these critical values approximate injury thresholds. The critical values for compression (Fzc) and flexion (Myco) are summarized in Table III.

Due to the limited availability of PMHS cases in tension and extension modes for the selected cases, the critical values for these loading conditions would not be meaningful, as their magnitudes are significantly below actual injury thresholds. The observed values primarily reflect rebound effects from dominant compression or flexion loading. Further analysis will be required when more PMHS data for tension and extension tests become available.

In this study, a linear scaling approach was applied using the ratios from the HIII 50th percentile dummy (HIII-50M) for tension/compression forces in Fz and flexion/extension moments in My to estimate the THOR-AV neck tension Fz and extension moment My critical values. The THOR dummy's neck values were not used for scaling due to its unique design, incorporating front and rear neck cables. The calculations for the Fzc in tension and Myoc in extension are calculated as follows:

$$\text{Fzc in tension} = (6{,}807/6{,}160)*9{,}223 = 10{,}965 \text{ N} \tag{5}$$

$$\text{Myoc in extension} = (135/310)*119 = 52 \text{ Nm} \tag{6}$$

The summary of the critical values used for Nij calculations is provided in Table III.

TABLE III
SUMMARY OF CRITICAL VALUES FOR HIII-50M, THOR AND THOR-50M

		HIII-50M (FMVSS 208)	THOR (Proposed US NCAP)	THOR-AV (IARV at 50% injury risk)
Fzc	Tension (N)	6,807	4,200	10,965 (scaled from HIII-50M)
	Compression (N)	6,160	4,520	9,223
Myoc	Flexion (Nm)	310	60	119
	Extension (Nm)	135	79.2	52 (scaled from HIII-50M)

III. RESULTS

The shape, scale, quality index, GKG, AUROC and injury assessment risk values are summarised in Table IV. For neck AIS2+ compression force Fz, the IARVs corresponding to 5%, 25% and 50% injury risks are 2224 N, 5705 N and 9223 N, respectively. For neck AIS3+ compression force Fz, the IARVs at these injury risk levels are 3404 N, 9241 N and 15380 N, respectively.

For AIS2+ neck flexion moment Myoc at the OC joint, the IARVs at 5%, 25% and 50% injury risks are 12.5 Nm, 55.7 Nm, and 119.2 Nm, respectively. For AIS3+ neck flexion moment Myoc at OC joint, the corresponding IARVs are 20.1 Nm, 114.8 Nm and 279.1 Nm, respectively.

TABLE IV
SUMMARY OF SHAPE, SCALE, QUALITY INDEX, GKG, AUROC AND IARVS FOR THOR-AV NECK

MAIS	Predictor	Shape	Scale	Qual. Index	GKG	AUROC	IARVs 5%	IARVs 25%	IARVs 50%
AIS2+	Compression Fz (N)	1.8305	11267.6603	0.22	0.15	0.57	2224	5705	9223
	Flexion Myoc (Nm)	1.1562	163.6514	0.35	0.29	0.65	12.5	55.7	119.2
	Extension Myoc (Nm)	0.3920	24.2010	1.02	-0.51	0.25	0.01	1.01	9.50
	Nij	1.7583	2.6454	0.23	0.08	0.54	0.49	1.30	2.15
AIS3+	Compression Fz (N)	1.7263	19017.8646	0.35	0.11	0.55	3404	9241	15380
	Flexion Myoc (Nm)	0.9900	404.0723	0.62	0.00	0.50	20.1	114.8	279.1
	Extension Myoc (Nm)	0.2876	536.6418	2.20	-0.33	0.34	0.0	7.1	150.0
	Nij	1.4681	4.8489	0.42	-0.04	0.48	0.64	2.08	3.78

The injury risk curves (IRCs) were developed using the Weibull distribution for neck compression force Fz, moment Myoc at occipital condyle in both flexion and extension, and Nij for MAIS2+ and MAIS3+ injury levels. The IRC plots for AIS2+ injury risks are presented in Figs 3–6.

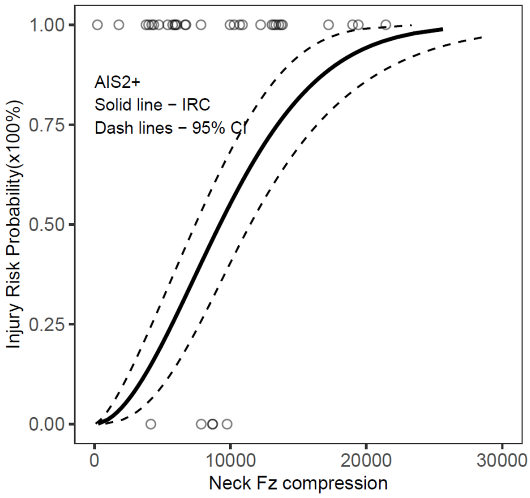

Fig. 3. IRC for upper neck compression force Fz (AIS2+).

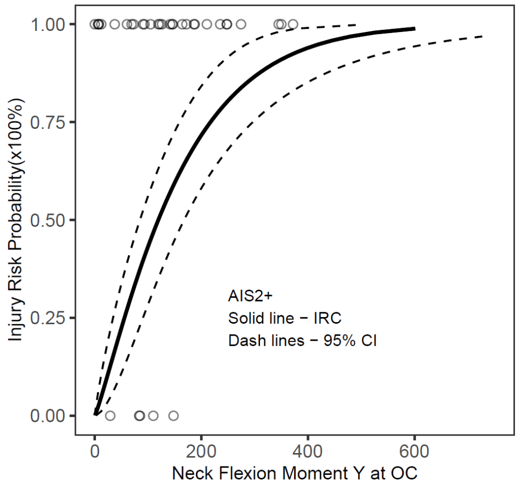

Fig. 4. IRC for upper neck flexion moment My at OC joint (AIS2+).

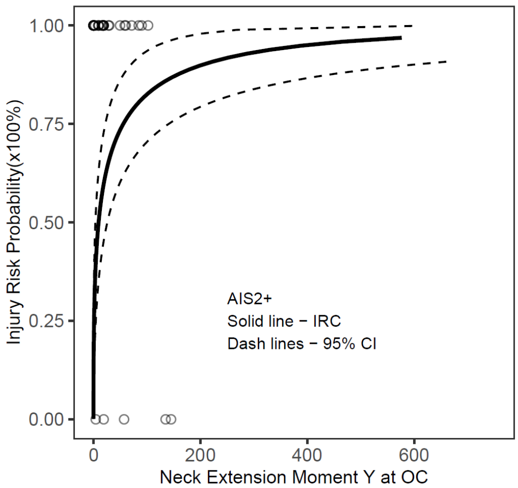

Fig. 5. IRC for upper neck extension moment Y at OC (AIS2+).

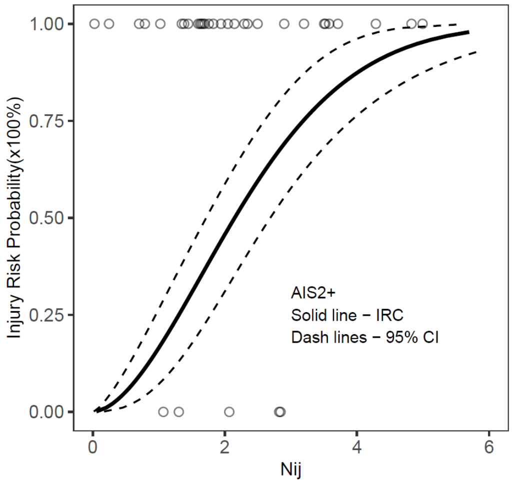

Fig. 6. IRC for upper neck Nij (AIS2+).

The IRCs for AIS3+ injury levels were also developed using the Weibull distribution for neck compression force Fz, moment Myoc at the occipital condyle in both flexion and extension, and Nij. The corresponding IRC plots for AIS3+ are presented in Figs 7–10.

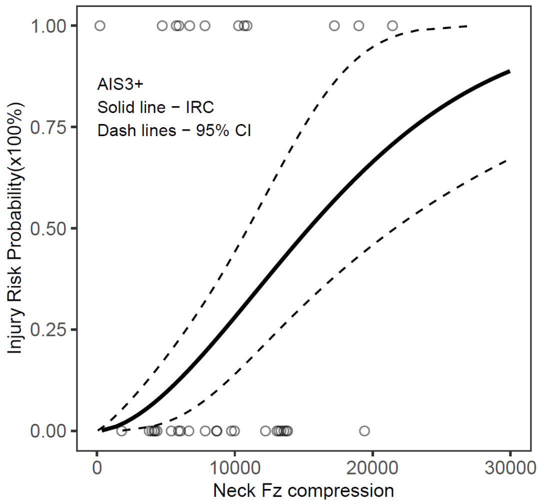

Fig. 7. IRC for neck compression Fz (AIS3+).

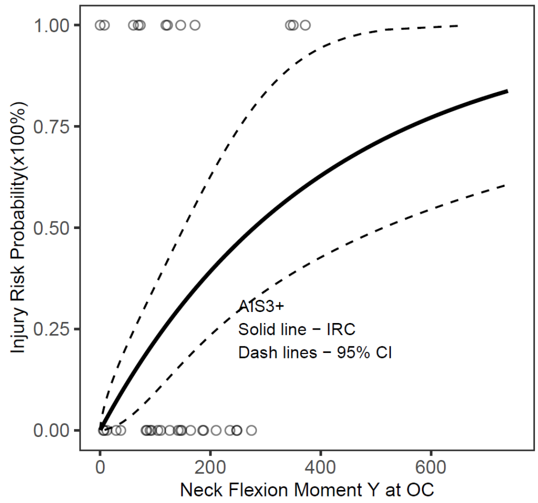

Fig. 8. IRC of neck flexion moment Y at OC (AIS3+).

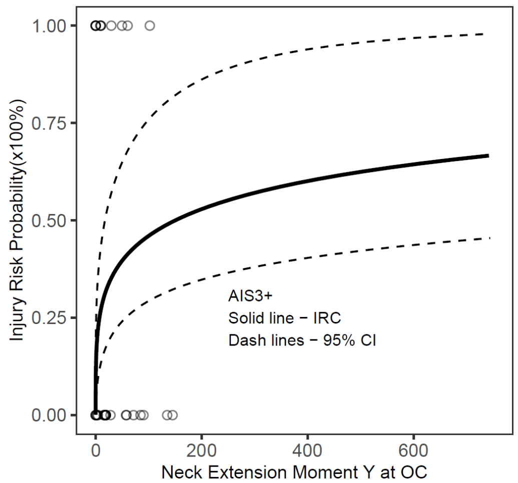

Fig. 9. IRC for neck extension moment Y at OC (AIS3+).

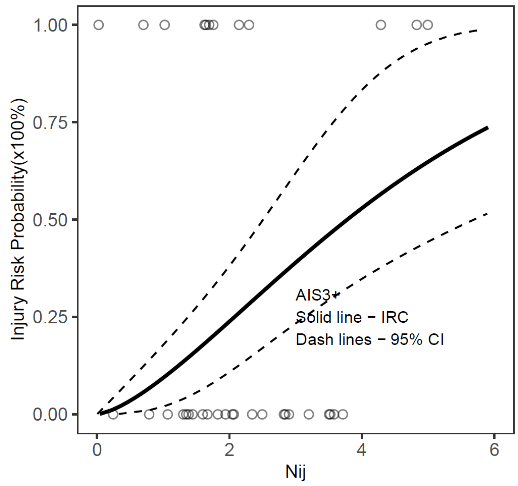

Fig. 10. IRC for neck Nij (AIS3+).

The Quantile-Quantile (QQ) plots were utilised to assess the quality of the survival model fit. For AIS2+ injury levels, the QQ plots for neck compression force Fz, neck flexion and extension moments in the y-direction Myoc, and Nij are displayed in Figs 11–14.

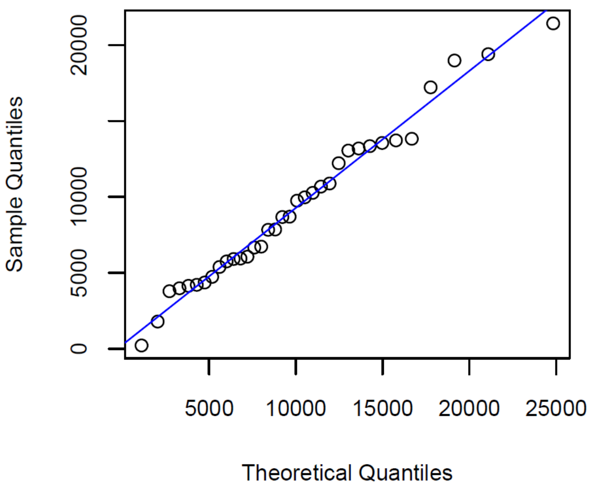

Fig. 11. QQ plot for neck compression (AIS2+).

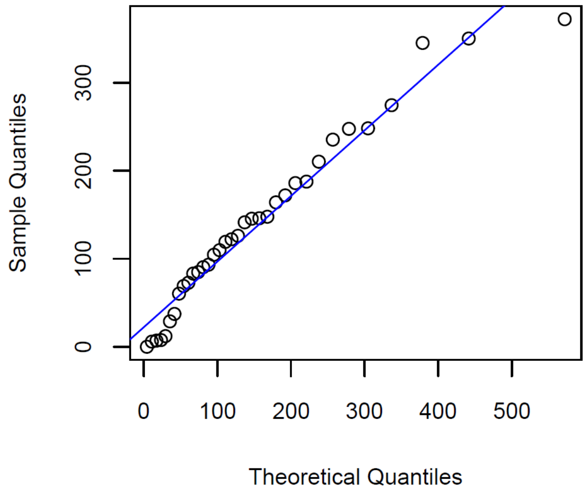

Fig. 12. QQ plot for neck flexion moment in y-direction (AIS2+).

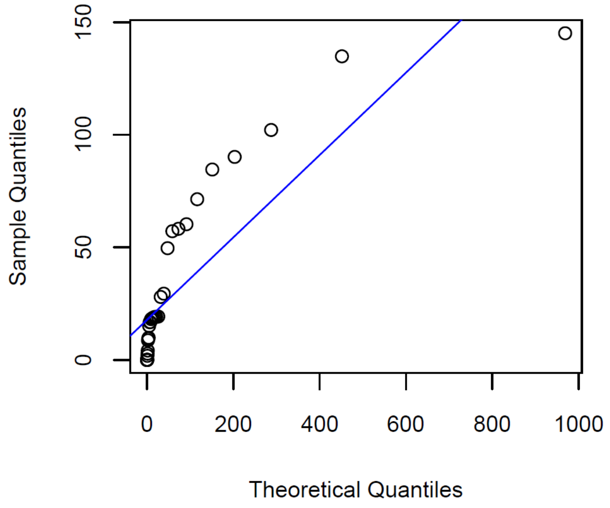

Fig. 13. QQ plot of neck extension moment in y-direction (AIS2+).

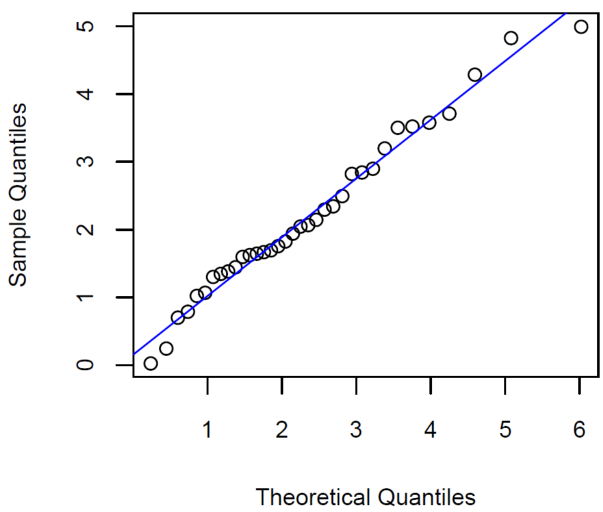

Fig. 14. QQ plot of neck Nij (AIS2+).

For AIS3+ injury level, the QQ plots for neck compression Fz, neck flexion and extension moments in y-direction Myoc, and Nij are presented in Figs 15–18.

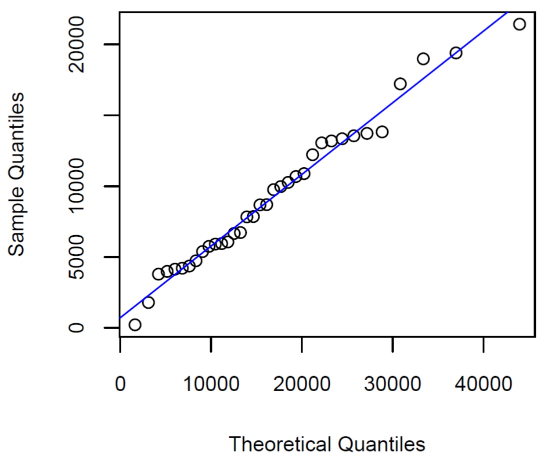

Fig. 15. QQ plot of neck compression force in z-direction (AIS3+).

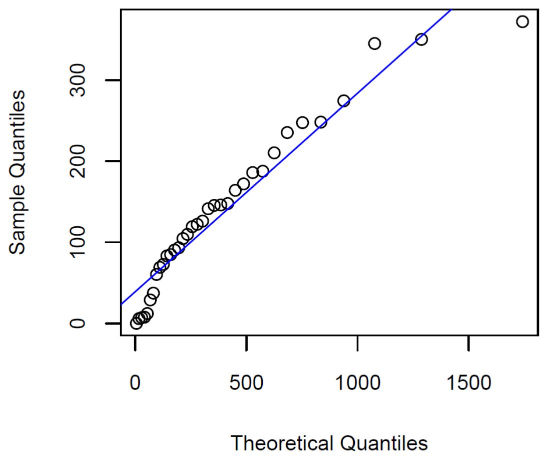

Fig. 16. QQ plot of neck flexion moment in y-direction (AIS3+).

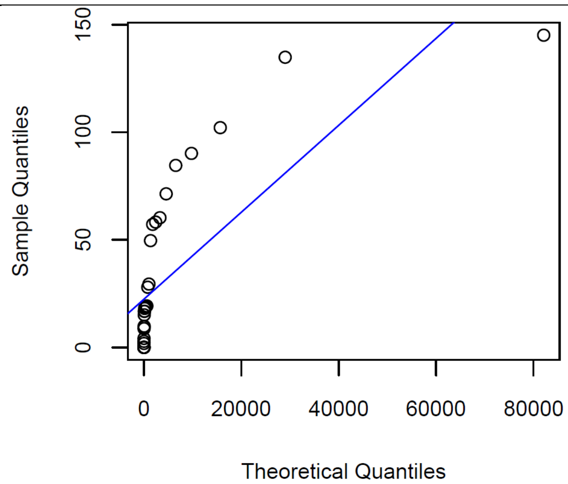

Fig. 17. QQ plot of neck extension force in z-direction (AIS3+).

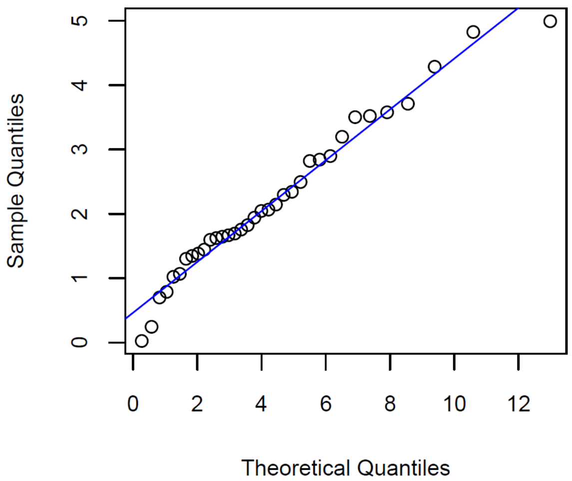

Fig. 18. QQ plot of neck Nij (AIS3+).

IV. DISCUSSION

THOR-AV upper neck IRCs were developed in this research, with only a small subset of published PMHS data deemed suitable. Some studies lacked sufficient details on boundary conditions, making them unusable for this analysis.

For all studies, the Goodman-Kruskal Gamma (GKG) values were observed to be low, with values of 0.15 for neck compression force Fz, 0.29 for upper neck moment Myoc, and 0.24 for Nij at AIS2+. The corresponding AUROC values for these predictors were 0.57, 0.65, and 0.62, indicating moderate predictive capability. However, the quality indices for these three predictors – 0.22, 0.35, and 0.19 – were excellent. The QQ plots shown in Fig. 9, Fig. 11, and Fig. 12 demonstrated a reasonable comparison between theoretical and sample quantiles.

It was also noted that neck extension moment Myoc at the occipital condyle performed poorly as an injury predictor, exhibiting negative GKG, low AUROC, and poor QQ comparisons. This is likely due to the predominance of compression, flexion, or combined compression-flexion load cases in this study, with an insufficient number of extension load cases to provide meaningful statistical analysis.

Given these findings, only neck compression force and flexion moment at the occipital condyle joint are recommended for injury assessment, while Nij should be used as a reference measure for compression and/or flexion predominant cases. These recommendations are summarised in Table V.

TABLE V
RECOMMENDATION FOR THOR-AV NECK INJURY RISK ASSESSMENT VALUES

MAIS	Predictor	Shape	Scale	IARVs 5%	25%	50%
AIS2+	Compression Fz (N)	1.8305	11267.6603	2224	5705	9223
	Flexion Myoc (Nm)	1.1562	163.6514	12.5	55.7	119.2
	Nij*	1.7583	2.6454	0.49	1.30	2.15
AIS3+	Compression Fz (N)	1.7263	19017.8646	3404	9241	15380
	Flexion Myoc (Nm)	0.9900	404.0723	20.1	114.8	279.1
	Nij*	1.4681	4.8489	0.64	2.08	3.78

*Nij values are for flexion- and/or compression-dominated load cases due to the PMHS load cases used for the IRC analysis in this study. It should not be used for extension- and/or tension-dominated cases.

There are a couple of limitations in this study. The PMHS specimens were mostly elderly, which would likely make the results conservative for an average 45-year-old male that THOR-AV represents. Tension/flexion loading IRCs were unfortunately not developed in this study, however, it is one of the dominant loading mechanisms for injuries in frontal crashes. There is no data to estimate the neck tension and flexion critical values, which were scaled from HIII 50th male dummy in this study.

V. CONCLUSIONS

Injury risk curves were analysed for the THOR-AV neck, with FE simulations conducted to generate matched-pair data corresponding to PMHS test conditions. The absence of PMHS test cases for tension and extension limited this study's recommendations to IARVs for neck compression and flexion only.

For AIS2+, the IARVs for neck compression were determined to be 2,224 N, 5,705 N, and 9,223 N at 5%, 25%, and 50% injury risk levels, respectively. The IARVs for flexion moment at the OC joint were 12.5 Nm, 55.7 Nm, and 119.2 Nm at the same injury risk levels. For AIS3+, the IARVs for neck compression were 3,404 N, 9,241 N, and 15,390 N, while the IARVs for flexion moment at the OC joint were 20.1 Nm, 114.8 Nm, and 279.1 Nm at 5%, 25%, and 50% injury risk levels, respectively.

Critical values were selected based on the 50% injury risk level for AIS2+ injuries. The IARVs for Nij at AIS2+ were 0.49, 1.30, and 2.15 at 5%, 25%, and 50% injury risk levels, respectively, while for AIS3+ the corresponding values were 0.63, 2.08, and 3.78. The Nij injury risk curves were derived from flexion and/or compression cases and may not represent extension and/or tension-dominated cases.

Currently, no field data are available for verification of these results, and caution should be exercised when applying these values to restraint system evaluations.

VI. ACKNOWLEDGEMENTS

The authors would like to express their gratitude to the Humanetics executive team for granting them the opportunity to dedicate time to conduct this research. The opinions expressed in this paper are solely those of the authors and may not reflect the views of their affiliated organisation.

VII. REFERENCES

[1] Jorlöv, J., Bohman, K., Larsson, A., (2017) Seating positions and activities in highly automated cars – a quantitative study of future automated driving scenarios. *Proceedings of the* IRCOBI Conference, 13–15 September 2017, Antwerp, Belgium.

[2] Wang, Z. J., Lober, B., Tesny, A., Hu, G., Kang, Y-S. (2021) Neck biofidelity comparison of THOR-AV, THOR and Hybrid III 50th dummies. *Proceedings of the IRCOBI Conference*, 8–10 September 2021, online.

[3] Wang, Z. J., Richard, O., *et al*. (2022a) Biomechanical responses of THOR-AV in a semi-rigid seat that mimics the front and rear seat of a midsize car. *Proceedings of the IRCOBI Conference*, 14–16 September 2022, Porto, Portugal.

[4] Wang, Z. J., Zaseck, L. W., Reed, M. P. (2022b) THOR-AV 50th percentile male biofidelity in 25° and 45° seatback angle test conditions with a semi-rigid seat. *Proceedings of the IRCOBI Conference*, 14–16 September 2022, Porto, Portugal.

[5] Wang, Z. (2022) Biomechanical responses of the THOR-AV ATD in rear racing test conditions. *SAE International Journal of Advances and Current Practices in Mobility,* **4**(6): pp. 2089–2105. https://doi.org/10.4271/2022-01-0836.

[6] Wang, Z. J., He, G. (2024) Investigation of injury risk functions of THOR-AV 50th percentile male dummy. *Stapp Car Crash Journal*, vol. **68**, 2024.

[7] ISO/TS 18506:2014 (2014) Procedure to construct injury risk curves for the evaluation of the road user protection in crash tests (Edition 1, 2014).

[8] Alem, N., Nusholtz, G., Melvin, J. (1984) Head and neck response to axial impacts, SAE Technical Paper 841667, 1984, https://doi.org/10.4271/841667.

[9] Yoganandan, N., Sances, A. Jr, *et al.* (1986) Experimental spinal injuries with vertical impact. *Spine* (Phila Pa 1976), **11**(9): pp. 855–860. doi: 10.1097/00007632-198611000-00001. PMID: 3824059.

[10] McElhaney, J., Doherty, B., *et al*. (1988) Combined bending and axial loading responses of the human cervical spine. SAE Technical Paper 881709, 1988, https://doi.org/10.4271/881709.

[11] Nightingale, R., Doherty, B., *et al*. (1991) The Influence of end condition on human cervical spine injury mechanisms. SAE Technical Paper 912915, 1991, https://doi.org/10.4271/912915.

[12] Pintar, F., Yoganandan, N., *et al*. (1995) Dynamic characteristics of the human cervical spine. SAE Technical Paper 952722, 1995, https://doi.org/10.4271/952722.

[13] Yoganandan, N., Sances, A. Jr, *et al*. (1990) Injury biomechanics of the human cervical column. *Spine* (Phila Pa 1976), **15**(10): pp. 1031–1039. doi: 10.1097/00007632-199015100-00010. PMID: 2263968.

[14] McElhaney, J., Paver, J., McCrackin, H., Maxwell, G. (1983) Cervical spine compression responses. SAE Technical Paper 831615, 1983, https://doi.org/10.4271/831615.

[15] Pintar, F., Yoganandan, N., *et al*. (1989) Kinematic and anatomical analysis of the human cervical spinal column under axial loading. SAE Technical Paper 892436, 1989, https://doi.org/10.4271/892436.

[16] Pintar, F., Sances, A. Jr, *et al*. (1990) Biodynamics of the total human cadaveric cervical spine. SAE Technical Paper 902309, 1990, https://doi.org/10.4271/902309.

[17] Yoganandan, N., Pintar, F. A., Sances, A. Jr, Reinartz, J., Larson, S. J. (1991) Strength and kinematic response of dynamic cervical spine injuries. *Spine* (Phila Pa 1976), **16**(10 Suppl): pp. S511–S517. doi: 10.1097/00007632-199110001-00011. PMID: 1801263.

[18] Nightingale, R. W., McElhaney, J. H., Richardson, W. J., Best, T. M., Myers, B. S. (1996) Experimental impact injury to the cervical spine: relating motion of the head and the mechanism of injury. *Journal of Bone and Joint Surgery Am*, **78**(3): pp. 412–421. doi: 10.2106/00004623-199603000-00013. PMID: 8613449.

[19] Nightingale, R., McElhaney, J., *et al*. (1997) The dynamic responses of the cervical spine: buckling, end conditions, and tolerance in compressive Impacts. SAE Technical Paper 973344, 1997, https://doi.org/10.4271/973344.

[20] Wismans, J. and Spenny, C. H. (1983) Performance requirements for mechanical necks in lateral flexion. Proceedings of 27th Stapp Car Crash Conference, SAE paper No. 831613, Warrendale, PA 15096, pp. 137–148.

[21] Thunnissen, J., Wismans, J., Ewing, C. L., Thomas, D. J. (1995) Human Volunteer Head-Neck Response in Frontal Flexion: A New Analysis. Thirty-ninth Stapp Car Crash Conference, San Diego, California, 8–10 November 1995, SAE Paper # 952721.

[22] Kang, Y-S., Stammen, J., Moorhouse, K., Bolte, J. (2018) Head and neck responses of post-mortem subjects in frontal, oblique, side and twist scenarios. *Proceedings of the IRCOBI) Conference*, 12–14 September 2018, Athens, Greece.

[23] Lee, E. L., Parent, D. P., Craig, M. J., McFadden, J., Moorhouse, K. (2017) Biomechanical response requirements manual – THOR 5th percentile female, NHTSA advanced frontal dummy. US Department of Transportation, National Highway Traffic Safety Administration, DOT HS 812 370, February 2017.

[24] Eppinger, R. H., Marcus, J. H., Morgan, R. M. (1984) Development of dummy and injury index for NHTSA's thoracic side impact protection research program. SAE Technical Paper# 840885, https://doi.org/10.4271/840885.

[25] ISO/TS 18506 (2014) Procedure to construct injury risk curves for the evaluation of the road user protection in crash tests (Edition 1, 2014).

[26] Eppinger, R., Sun, E., *et al*. (1999) Development of improved injury criteria for the assessment of advanced automotive restraint systems–II. Washington, DC: National Highway Traffic Safety Administration. https://ntrl.ntis.gov/NTRL/dashboard/searchResults/titleDetail/PB2002104560.xhtml#.

[27] FMVSS 208 S6.6 Neck injury, https://www.ecfr.gov/current/title-49/subtitle-B/chapter-V/part-571/subpart-B/section-571.208.

[28] Craig, M., Parent, D., *et al*. (2019) Injury criteria for the THOR 50th male ATD. NHTSA docket #: NHTSA-2019-0106, https://www.regulations.gov/document/NHTSA-2019-0106-0008.

[29] Takhounts, E. G., Craig, M. J., Moorhouse, K., McFadden, J., (2013) Development of brain injury criteria (BrIC). *Stapp Car Crash Journal*, **57**(November 2013): pp. 243–266.

[30] Mertz, H. J. (1993) *Anthropomorphic test devices, Accidental Injury: Biomechanics and prevention*. Springer: New York, NY, USA.

[31] Kuppa, S., Wang, J., Haffner, M., Eppinge,r R. (2001) Lower extremity injuries and associated injury criteria. 17th ESV Conference Proceedings, 4–7 June 2001, Amsterdam, The Netherlands.

APPENDIX

TABLE A1

LIST OF SPECIMENS, LOADING MODE, SEX, AGE, MAIS AND LOAD SPEED

Reference	Specimen #	Vertebra #	Loading Mode	Sex	Age	MAIS	Load Vel (m/s)
McElhaney et al. 1983	A79-409	BOS* to T2	Comp-Flx	M	58	2	0.5
	A79-415	BOS to T1	Comp-Flx	M	37	2	0.5
	A79-423	BOS to T1	Comp-Flx	M	52	2	0.5
	A79-431	BOS to T1	Comp-Flx	M	46	2	0.5
	A80-289	BOS to T1	Comp-Flx	M	70	2	0.54
	A80-352	BOS to C6	Comp-Flx	M	62	2	0.55
	A80-364	BOS to C6	Comp-Flx	M	41	2	0.45
	A80-368	BOS to C6	Comp-Flx	M	77	2	0.57
	A83-26	C2 to C7	Comp-Flx	M	44	3	0.88
Pintar et al. 1989	201	C1-T1	Compression	M	66	2	2
	202	C1-T1	Compression	M	69	3	2
	203	C1-T1	Compression	M	-	3	2
	204	C1-T1	Compression	M	72	3	2
	205	C1-T1	Compression	M	65	2	2
	206	C1-T1	Compression	M	66	3	2
	207	C1-T1	Compression	M	59	3	2
Pintar et al. 1990	4	C1-T1	Compression	M	50	2	8.13
Yoganandan et al. 1991	4:4495	full neck	Compression	M	50	2	8.5
	9599D	full neck	Compression	M	50	3	5.8
	377-7	full neck	Compression	M	69	3	7.8
	H8205	full neck	Compression	M	48	2	5.4
Nightingale et al. 1997 Stapp	N05-R+30	head/neck	Ext-Com	M	36	2	3.23
	N18-R +15	head/neck	Ext-Com	M	-	3	3.26
	D41-R +15	head/neck	Ext-Com	M	69	0	3.11
	I32-R +15	head/neck	Ext-Com	M	78	2	3.18
	N26-R +0	head/neck	Compression	M	65	0	2.43
	N22-R +0	head/neck	Compression	M	62	3	3.2
	N24-R +0	head/neck	Compression	M	71	3	3.26
	N11-R -15	head/neck	Flx-Com	M	55	0	3.14
	UK3-R -15	head/neck	Flx-Com	M	62	0	3.13
	N21-P+30	head/neck	Ext-Com	M	61	2	3.13
	N23A+30	head/neck	Ext-Com	M	46	1	3.03
	N23B-P+30	head/neck	Ext-Com	M	46	2	3.51
	I08-P -15	head/neck	Flx-Com	M	80	2	3.15
	I04-P +15	head/neck	Ext-Com	M	63	2	3.19
	N03-P +0	head/neck	Compression	M	75	3	3.08
	NA2-P -15	head/neck	Flx-Com	M	61	2	3.16
	I26-P -15	head/neck	Flx-Com	M	59	2	3.07

*BOS – bottom of the skull

TABLE A2

SCALED OR NON-SCALED VALUES FOR THE IRC DEVELOPMENT

Ref	specimen #	weight (kg)	stature (cm)	Fx_ max	Fx_ min	Fz_ max	Fz_ min	My_ max	My_ min	Mxoc_ max	Mxoc_ min	Myoc_ max	Myoc_ min	Nij_ max	scaled
McElhaney et al. 1983	A79-409/415/423	-	-	3482	-668	2468	-13724	360.4	-4.7	20.9	-14.9	274.4	-16.8	3.71	No
	A80-289	-	-	2030	-721	2671	-13555	308.5	-5.1	22.6	-16.1	248.2	-18.1	3.52	No
	A80-352	-	-	2194	-735	2721	-13829	308.7	-5.2	23.0	-16.4	247.5	-18.4	3.58	No
	A80-364	-	-	1775	-601	2216	-12223	238.7	-4.2	18.8	-13.5	187.7	-15.1	2.90	No
	A80-368	-	-	2068	-762	2821	-13193	261.6	-5.4	23.8	-17.0	210.3	-19.1	3.20	No
	A83-26	-	-	6403	-1176	4368	-17220	474.3	-8.2	36.7	-26.1	372.0	-29.4	4.99	No
Pintar et al. 1989	201	45	173	201	0	0	-1791	12.1	0.0	0.0	0.0	6.0	0.0	0.25	Yes
	202	82	170	1314	-1	0	-7834	211.3	0.0	0.2	-0.1	172.0	0.0	2.30	Yes
	203	54	173	683	0	0	-4736	81.0	0.0	0.0	-0.1	60.5	0.0	1.02	Yes
	204	75	170	1062	-1	0	-6726	154.1	0.0	0.1	-0.1	122.2	0.0	1.76	Yes
	205	88	178	524	-1	0	-4361	53.2	0.0	0.0	0.0	37.5	0.0	0.79	Yes
	206	45	157	1006	0	0	-5751	149.3	0.0	0.3	-0.7	119.3	0.0	1.62	Yes
	207	68	173	23	-1	0	-216	0.9	0.0	0.1	-0.1	0.2	0.0	0.03	Yes
Pintar et al. 1990	4	75	178	3680	-24	7	-13054	288.7	-0.7	6.7	-10.6	186.0	-1.8	2.50	Yes
	4:4495	75	178	3806	-770	2872	-13346	277.4	-39.6	6.7	-2.8	164.2	-16.8	2.34	Yes
	9599D	82	175	4953	-381	53	-21432	466.9	-113.3	6.1	-12.8	345.0	-102.1	4.83	Yes
	377-7	68	178	6275	-1548	184	-18988	524.8	-94.5	4.5	-10.5	350.1	-49.6	4.29	Yes
	H8205	82	183	4073	-1	3	-19404	357.7	0.0	5.1	-6.1	235.3	0.0	3.50	Yes
Nightingale et al. 1997 Stapp	N05-R+30	-	-	1673	-387	680	-6667	152.8	-79.0	1.8	-1.5	104.7	-71.4	1.60	No
	N18-R +15	-	-	1997	-394	754	-10269	182.0	-70.7	2.3	-3.9	146.1	-60.3	2.14	No
	D41-R +15	-	-	2032	-348	624	-9754	191.9	-66.2	1.6	-2.9	147.8	-57.2	2.07	No
	I32-R +15	-	-	2082	-366	707	-9973	186.7	-68.3	2.7	-3.1	145.5	-58.2	2.05	No
	N26-R +0	-	-	1123	-346	1040	-7853	62.7	-13.8	1.4	-1.8	29.0	-4.2	1.07	No
	N22-R +0	-	-	1880	-575	1391	-10885	129.0	-25.7	2.5	-2.9	72.8	-9.5	1.69	No
	N24-R +0	-	-	1831	-573	1381	-10682	124.0	-25.9	2.4	-2.8	69.1	-9.9	1.65	No
	N11-R -15	-	-	1345	-1758	605	-8698	92.8	-197.9	3.1	-2.8	85.0	-145.1	2.84	No

Ref	specimen #	weight (kg)	stature (cm)	Fx_ max	Fx_ min	Fz_ max	Fz_ min	My_ max	My_ min	Mxoc_ max	Mxoc_ min	Myoc_ max	Myoc_ min	Nij_ max	scaled
	UK3-R -15	-	-	1332	-1631	548	-8677	90.8	-178.1	2.3	-2.3	83.3	-134.8	2.82	No
	N21-P+30	-	-	893	-48	62	-3790	152.9	-4.2	0.2	-1.2	126.2	-2.8	1.44	No
	N23A+30	-	-	907	0	57	-4144	134.1	-18.3	0.4	-0.2	109.8	-19.1	1.30	No
	N23B-P+30	-	-	1125	-29	76	-5385	172.2	-28.1	1.5	-3.6	141.5	-28.0	1.67	No
	I08-P -15	-	-	639	-102	46	-5911	109.2	-21.7	0.5	-0.6	90.5	-18.7	1.35	No
	I04-P +15	-	-	658	-105	52	-6065	112.4	-22.3	0.6	-0.7	93.3	-19.3	1.38	No
	N03-P +0	-	-	561	-150	4	-5944	23.6	-12.9	0.6	-0.3	7.8	-8.7	0.70	No
	NA2-P -15	-	-	368	-490	0	-4212	6.3	-103.4	0.3	-0.2	7.2	-90.1	1.94	No
	I26-P -15	-	-	318	-469	0	-3983	12.1	-97.5	0.3	-0.3	12.3	-84.6	1.83	No

Specimen weight and stature with "-" are not reported in the original publications.